http://dx.doi.org/10.5935/0103-5053.20130306

*J. Braz. Chem. Soc.*, Vol. 25, No. 3, 418-426, 2014.
Printed in Brazil - ©2014 Sociedade Brasileira de Química
0103 - 5053 $6.00+0.00

Review

# Nanoparticle Mediated Electron Transfer Across Organic Layers: From Current Understanding to Applications

*J. Justin Gooding,* Muhammad Tanzirul Alam, Abbas Barfidokht and Lachlan Carter*

*School of Chemistry and Australian Centre for NanoMedicine, The University of New South Wales, Sydney, NSW 2052, Australia*

Nos últimos anos, montagens do tipo eletrodo-camada orgânica-nanopartícula têm atraído interesse de pesquisa considerável para sistemas onde o eletrodo é passivado na ausência das nanopartículas. Isso acontece porque tem-se observado que se a camada orgânica for uma boa monocamada auto-montada para passivar o eletrodo, a presença de nanopartículas "ligam" a eletroquímica faradaica, e porque a transferência de elétrons entre o eletrodo e as nanopartículas é aparentemente independente da espessura da camada orgânica. Este *review* 1) destaca quão importante são as observações experimentais a respeito deste fenômeno, 2) discute uma descrição teórica recente para explicar as observações que acabaram de ser apoiadas por evidências experimentais e 3) fornece um resumo sobre a aplicação desses sistemas em sensores e sistemas fotovoltaicos.

In the last few years electrode-organic layer-nanoparticle constructs have attracted considerable research interest for systems where in the absence of the nanoparticles the electrode is passivated. This is because it has been observed that if the organic layer is a good self-assembled monolayer that passivates the electrode, the presence of the nanoparticles "switches on" faradaic electrochemistry and because electron transfer between the electrode and the nanoparticles is apparently independent of the thickness of the organic layer. This review 1) outlines the full extent of the experimental observations regarding this phenomenon, 2) discusses a recent theoretical description to explain the observations that have just been supported with experimental evidences and 3) provides an overview of the application of these systems in sensing and photovoltaics.

**Keywords:** nanoparticles, electron transfer across insulation layer, self-assembled monolayer, HbA1c sensor, quantum dot sensitized solar cells

## 1. Introduction

The modification of electrodes with nanoparticles has been the subject of thousands of papers[1] but one of the most curious observations is that of nanoparticle mediated charge transfer. This term has arisen for electrode-insulator-nanoparticle constructs. In the absence of the nanoparticles, the insulating layer passivates the electrode such that no appreciable Faradaic electrochemistry between the electrode and a redox species in solution proceeds. However, upon binding of nanoparticles to the surface of the insulating layer, efficient charge transfer across the insulating layer is observed. This phenomenon was first reported in the mid-1990s by Natan and co-workers[2,3] where gold or silver nanoparticles were covalently attached to a polymerized silane modified platinum electrode. They showed, with methyl viologen as a redox probe in solution, that the silane polymer passivated the electrode but that upon immobilisation of the nanoparticles onto the polymer layer efficient electron transfer was restored.

At around the same time, Schiffrin and co-workers[4-6] reported a similar phenomenon using alkyl dithiols to link electrodes to nanoparticles. Again the onset of electrochemistry at an otherwise blocking organic layer was observed with these assemblies when nanoparticles were attached. Furthermore, Schiffrin and co-workers[6] showed that if multilayer assemblies were fabricated in a stepwise manner, each time the assembly was terminated with the alkyl dithiol the Faradaic electrochemistry was suppressed and each time the assembly was terminated with nanoparticles distinct Faradaic electrochemistry was observed for $[Fe(CN)_6]^{3-/4-}$ in solution. Since then

*e-mail: justin.gooding@unsw.edu.au

similar observations have been reported with different electrode types including gold,[3] platinum,[2,6] silicon,[7] carbon[8,9] and indium tin oxide[10,11] and with different types of nanoparticles including gold,[3] platinum,[6] silver,[10] carbon nanotubes,[12-14] cadmium telluride (CdTe) and cadmium selenide quantum (CdSe) dots.[15,16]

However, the phenomenon was essentially ignored until two papers in 2008 and 2009 from the Fermin[17] and Gooding[18] group, respectively. These papers raised such interest as they suggested the charge transfer between electrode and gold nanoparticles (AuNPs) was independent of the thickness of the organic monolayer. Such an observation was important both from a fundamental and an applied perspective. From a fundamental perspective such observations are so unexpected that they raise the question as to what is the mechanism that is occurring. From an applied perspective, electrode-organic layer-nanoparticle constructs suddenly allow the incredible power of modern nanoparticle synthesis to be exploited in electrochemistry on an otherwise low capacitance electrode. The electrode has low capacitance as the majority of the electrode is passivated. Placing nanoparticles onto the passivating layers therefore could have applications in electroanalysis, biosensing electrocatalysis, and even photovoltaic devices. In this short review we will discuss the basic observations from the Fermin[17] and Gooding[18] group, discuss the theoretical framework that has been established to explain these results and then overview some recent literature where electrode-organic layer-nanoparticle constructs have been applied.

## 2. The Key Observations

The surface constructs used in the papers by the Fermin group[9,17,19-21] and the Gooding group[18,22] are shown in Figure 1. Despite the differences the results are very similar. In the Fermin case, AuNPs-modified electrodes were fabricated by modifying a gold electrode with a carboxyl terminated alkanethiol self-assembled monolayer (SAM). Next, a polycationic poly-l-lysine layer, which possessed free amine groups, was adsorbed on the SAM. AuNPs were then attached to this electrode via the affinity of the free amines for nanoparticulate gold. $[Fe(CN)_6]^{3-/4-}$ was used as an anionic redox couple. In the absence of the nanoparticles any electrochemistry from the $[Fe(CN)_6]^{3-/4-}$ was blocked by the organic layer. However, when nanoparticles were attached to the organic layer two surprising observations were made. Firstly, electrochemistry from the $[Fe(CN)_6]^{3-/4-}$ that resembled that from a bare electrode was observed and secondly kinetics of charge transfer was independent of the length of the linking SAM. In fact, if the rate constant for electron transfer per particle was considered then the kinetics of electron transfer were found to be identical to bare gold.[17,18]

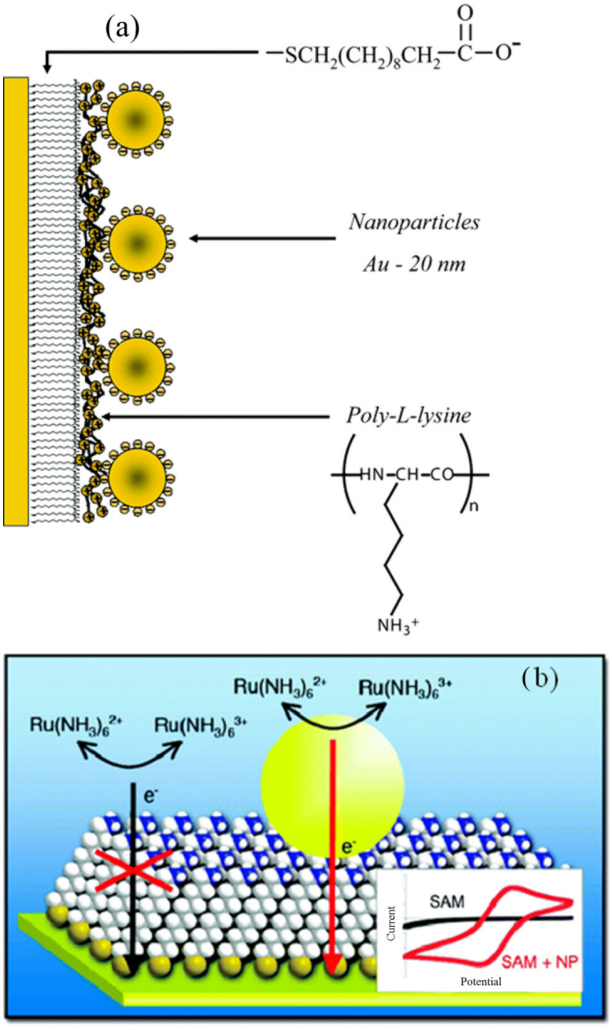


**Figure 1.** Schematics of the electrode constructs first used by a) Zhao *et al*. and b) Shein *et al.* where the observation of nanoparticle mediated charge transfer was characterised in detail (Adapted from references 21 and 18, respectively).

The electrode construct used in the Fermin work did however cause some ambiguity in relation to these observations and the mechanism by which the electrochemistry could be "switched on". In the Fermin work, once the nanoparticles were attached to the SAM via an intervening polyelectrolyte layer, the positively charged poly-l-lysine served to concentrate the anionic $[Fe(CN)_6]^{3-/4-}$ redox probe directly adjacent to the AuNPs. The Gooding papers[18,22] however discounted that the polyelectrolyte was the cause of these unexpected observations. They fabricated a simpler construct (Figure 1b) where the electrode was modified with amine-terminated alkanethiols such that the AuNPs could be attached directly to the SAM without

any polyelectrolyte. In this case the redox active species used was $[Ru(NH_3)_6]^{3+}$. Again the same observations were made, the presence of nanoparticles "switched on" the electrochemistry compared to when the electrode was only modified by the SAM and that the electron transfer kinetics appeared to be independent on the thickness of the SAM as shown in Figure 2.

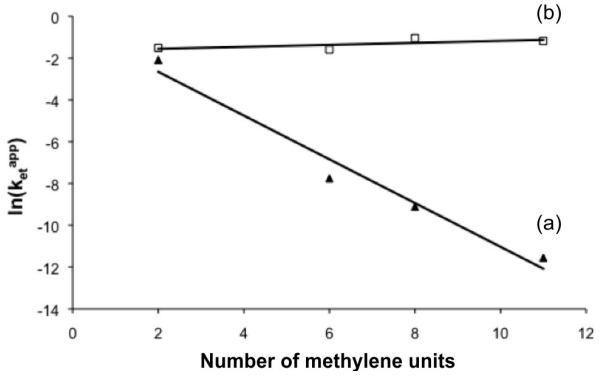


**Figure 2.** Variation in rate of electron transfer to $[Ru(NH_3)_6]^{+3}$ with the length of the alkanethiol linker for (a) electrodes modified with the SAM alone and (b) after nanoparticles were conjugated to the respective SAMs (Adapted from reference 18).

These observations were highly surprising as charge transfer through organics layers is expected to proceed via the super-exchange mechanism where the distance dependence of the electrode transfer rate constant ($k_S$) can be described by the equation

$$k_s = k^0 e^{-bd} \quad (1)$$

where $k^0$ is a pre-exponential factor, β is the attenuation factor (electron tunneling constant) and $d$ is the chain length which, for alkyl chains (electrode surface)–S-$(CH_2)_n$–(redox centre) is generally expressed in units of the number, $n$, of methylene groups, or alternatively the number of bonds, within the organic layer. So typically the apparent rate of electron transfer is expected to decay exponentially with the length of the organic molecules with a β value of between 0.8 and 1.1 $Å^{-1}$ as was observed for the SAM alone (Figure 2a). However, with the nanoparticles attached to the distal end of the SAM, the β value was zero (Figure 2b).

One possible explanation for these two surprising observations was that the nanoparticles are penetrating the SAM and forming a short circuit with the underlying electrode surface. Bharathi *et al.*,[23] who modified a gold electrode with a silica sol followed by addition of gold nanoparticles, came to the conclusion that the onset of electrochemistry was due to nanoparticles penetrating throughout the silica layer. With alkanethiol SAM however, it seems highly unlikely the nanoparticles could penetrate the SAM, as to get the blocking behaviour observed in Figure 2a requires a close packed SAM which is analogous to a two dimensional crystalline layer. Chazalviel and Allongue[24] provided a convincing argument to support the notion that the particles are on top of the SAM based on atomic force microscopy. The argument is that for an AFM tip to penetrate a SAM of 12 methylene carbons would require a force of 100 nN which is an order of magnitude greater than the maximum 10 nN van der Waals attractions between a 10 nm nanoparticle and a SAM. Dyne *et al.*[22] also addressed this very issue and used Raman spectroscopy that exploits gap-mode plasmon excitation[25] to show that at least the vast majority of nanoparticles are located on the distal end of the SAM. Neither of these results definitively shows the nanoparticles are on the distal end of the organic layer. However Zhao *et al.*[19] showed that even if there was a silicon dioxide layer between the electrode and the nanoparticles efficient charge transfer could proceed. Similarly, Barfidokht *et al.*[26] also showed that charge transfer across a polymer layer was possible and subsequently showed that polymer layers with significant defects showed quite different electrochemical behaviour.[27] Hence we feel the evidence is conclusive that the nanoparticles are sitting on the top of the organic layer rather than forming a 'short' to the underlying bulk electrode.

Regarding the apparent distance independence of charge transfer, Bradbury *et al.*[17] suggested this simply meant that the rate limiting step was not charge transfer through the organic layer (i.e., electronic coupling between the electrode and nanoparticles) rather the electron transfer process is limited by the charging of the metal nanoparticle by the redox active species. This notion is supported by Dyne *et al.*[22] where the nanoparticles were modified with short alkanethiols of different charge. Using a cationic $[Ru(NH_3)_6]^{3+}$ redox probe, the rate constant of electron transfer was shown to decrease as the particles became more cationic. That is, if the charge of the particles repelled the redox active species, the electron transfer kinetics was found to be slower. Note in this same paper the size of the nanoparticles, between 3.8 and 67 nm, was shown to have no effect on the electron transfer kinetics.

The effect of the nature of nanoparticles on their electronic coupling with the gold electrode is studied by Liu *et al.*[28] To carry out the study, they shifted the rate determining step from electron transfer between redox probe and nanoparticle (as observed with $[Ru(NH_3)_6]^{2+/3+}$ as redox couple) to the electronic coupling between the electrode and nanoparticle using surface bound 6-(ferrocenyl)hexanethiol as redox probe. The rate determining step shifted due to the higher rate of electron transfer of 6-(ferrocenyl) hexanethiol ($2.4 \times 10^6$ $s^{-1}$),[29] which is seven to eight orders

of magnitude larger than that of the $[Ru(NH_3)_6]^{2+/3+}$. The apparent electron transfer rates of their nanoparticle modified gold electrode depend on the nature of the NPs following AuNPs > PtNPs > PdNPs order, with the electron transfer rate around an order of magnitude lower for the PdNPs than for the AuNPs and PtNPs. Electrons transfer rate at PdNPs drop further an order of magnitude when the length of thiol chain (used as insulating layer) was increased from eight to ten carbon atoms whereas much smaller changes were observed for AuNPs and PtNPs indicating weaker electronic coupling of the PdNPs to the gold electrode surface via the insulating SAM.

### 2.1 Theoretical evidence to support the observations

The studies by the Fermin group and Gooding group provoked Chazalviel and Allongue to develop a theoretical description of the mechanism of the nanoparticle-mediated electron transfer.[24] The authors made the simple analogy with electron transfer between two metal phases being far easier than between a metal and a dilute redox species in solution. That is, the theory suggested effective nanoparticle-mediated electron transfer with distant independent rate of electron transfer as long as exchange current density across the SAM on metal/SAM/metal ($J_1$) assembly is much larger than that on a metal/SAM ($J_0$) assembly. The higher current density, $J_1$, in the case of a metal/SAM/metal is attributed to the higher density of states on the nanoparticle. The implication of this is, in the metal/organic layer case, the potential drops exponentially with distance across the insulating organic layer as in equation 2.

$$V = \frac{2k_B T}{q} \sinh^{-1}\left(\frac{J}{2J_0 \exp(-\beta d)}\right) \quad (2)$$

where $V$ is the overpotential, $T$ is absolute temperature, $k_B$ the Boltzmann's constant, $q$ the elementary charge, $J$ the current density, β the attenuation factor and $d$ the thickness of the organic layer. However, in the case of the metal/organic layer/nanoparticles constructs there are two contributions to the potential, the electrochemical interface and the potential drop across the insulating layer.

$$V = \frac{k_B T}{q}\left[2\sinh^{-1}\left(\frac{J}{2J_0}\right) + \frac{J}{J_1 \exp(-\beta d)}\right] \quad (3)$$

In the case of a large value of $J_1$, the second term related to the organic layer is negligible if $J_1 \exp(-\beta d)$ is greater than $J$ and $J_0$. If such a situation exists, then the result of metal/organic layer/nanoparticles is an effective short circuit where the potential applied to the electrode is located on the nanoparticles. Hence distant independent electron transfer is expected until this condition fails. Once this condition fails the electron transfer behaviour will be distant dependent. This condition fails with very small nanoparticles or thick organic layers. The transition from distant dependent to distant independent electron transfer behaviour in these systems is shown in Figure 3 and was determined by equation 4.

$$J_1 \exp(-\lambda / 4k_B T)\exp(-\beta d) = J_0 \quad (4)$$

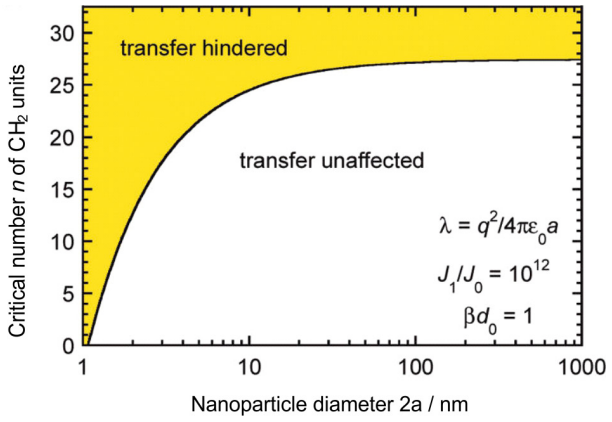


**Figure 3.** Critical number of $CH_2$ units of a bridging SAM above which gold nanoparticles are expected to lead to a change in the voltammogram of a reversible redox system in solution (shaded area) as compared to that obtained on a bare gold electrode. The black solid line shows the boundary between two regimes and the equation for this line is equation 4, where λ is the reorganization energy (Adapted from reference 24).

Barfidokht *et al.*[26] have recently provided experimental evidence to support this theory. The challenge was to find an organic system that could cover a wide enough spectrum of thicknesses such that the electron transfer kinetics could switch from the distance independent thickness regime to the distance dependent regime. This challenge arises because the thickness threshold above which the charge transfer kinetics becomes dependent on the thickness of the organic layer is greater than what can be achieved with SAM. In this case, the electrodeposited polymer, poly(ethylenediamine) was employed which was shown to give continuous thins films of thickness ranging from 6.6 Å to 38 Å as determined by ellipsometry. Barfidokht *et al.*[26] showed that up to a thickness of approximately 20 Å the kinetics of electron transfer were independent of the thickness of the polymer layer, thereafter the kinetics became dependent on the polymer layer thickness. That is the experimental study showed qualitative agreement with the theory (see Figure 4). The agreement is only qualitative because with an electrodeposited polymer there is likely to be varying thickness across the film and hence

the ellipsometry only gives an average thickness. Still the qualitative agreement is an important result as it provides a guide to the range of electrode modifications where thickness independent electron transfer kinetics can be obtained with electrode-organic layer-nanoparticle systems. Such knowledge is particularly important in applying this system to sensing, electrocatalysis and photovoltaics.

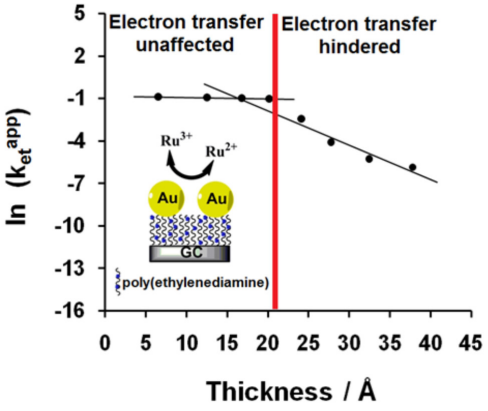


**Figure 4.** Influence of the thickness of organic layer on the nanoparticle mediated electrons transfer (Reprinted from reference 26. Copyright 2013 American Chemical Society).

## 3. Applications

### 3.1 Electroanalysis/sensing

Electrodes modified with passivating organic layers exhibit good Faradaic electrochemistry upon attachment of nanoparticles. Due to their low background capacitances, these constructs have good potential in electrochemical sensing. Electron transfer rate of metalloprotein, cytochrome *c*[30] and azurin,[31] confined to the AuNPs-SAM was reported to increase by more than an order of magnitude by Jensen *et al*. as compared to the nanoparticles free systems. AuNPs are considered to function as excellent electron transfer relays facilitating the electronic coupling between the protein redox site and the electrode surface.

Highly tuneable electrochemical interface was prepared by seeding growth of (3-mercaptopropyl) trimethoxysilane supported submonolayers of AuNPs via $NH_2OH$ reduction of $Au^{3+}$, where AuNPs behave as tuners of the electrochemical properties of the electrode interface.[32,33] The characteristic parameters (e.g., size and number density of the particles) of nanoelectrode arrays were finely tuned by combined controls of the synthesis of colloid, self-assembly, and surface-confined seeding growth in $Au^{3+}/NH_2OH$. The as-prepared nanoelectrode ensembles showed an adjustable sensitivity to heterogeneous electron-transfer kinetics, which is important from the perspective of sensor applications.[32,33] Su *et al*.[13] also reported similar observation where electrodes were prepared by controllable adsorption of the multiwalled carbon nanotube (MWNTs) onto SAM of *n*-octadecylmercaptan deposited onto gold electrodes. The adsorption of the MWNTs onto the SAM-modified gold electrode substantially restores heterogeneous electron transfer between gold electrode and redox species that was almost totally blocked by the SAM. The electrodes were found to have excellent electrochemical properties, such as tunable electrode dimensions from a nanoelectrode array to a conventional electrode and very small interfacial capacitance with good electrode activity.

Gooding *et al*.[34] have shown that ultra low limit of detection can be achieved in electrochemical sensing by a combined use of SAM and nanoparticles. Electrode was modified with SAM to lower the background current whereas AuNPs to the distal end of the SAM was attached to achieve electron transfer to the underlying electrode. Nanoparticles were also used in solution to complex the analyte and collect on the electrode. This principle was illustrated using cysteine-modified AuNPs for the accumulation and detection of Cu(II). The detection limit of the sensor was found to be 1 pmol $dm^{-3}$. Interfacial capacitance of the MWNT/SAM-modified gold electrode was also found to be considerably low as compared to the MWNT modified electrode prepared by directly confining MWNTs on to electrode surface.[13]

β-cyclodextrin/silver nanoparticles (AgNPs) composite modified low capacitive indium tin oxide electrodes were used to detect nitroaniline and chloronitrobenzene isomers by square wave voltammetry.[10] Different binding strengths of the nitroaromatic isomer to the β-cyclodextrin, and excellent electron transfer ability of AgNPs through passivating layer of β-cyclodextrin have enabled the selective detection of one isomer in presence of others (Figure 5). The proposed sensor was also used successfully in detecting nitroaromatic compounds in natural water samples. 4-(dimethylamino)pyridine capped AuNPs on top of 1,6-hexanedithiol modified gold electrode also showed enhanced lower limit of detection for the selective defection of 3,4-dihydroxyphenylacetic acid in the presence of ascorbic acid.[35]

An impedance-based immunosensor was constructed by Liu *et al*.[36] by modifying a gold electrode with 4-thiophenol passivating layers and subsequent attachment of gold nanoparticles. A biotin derivative was attached on top of this modified electrode to detect anti-biotin IgG. When the gold electrode was modified with 4-thiophenol, a significant increase in $R_{ct}$ was observed due to the formation of insulating organic layer. However, the $R_{ct}$ decreased noticeably after the immobilization of AuNPs on the

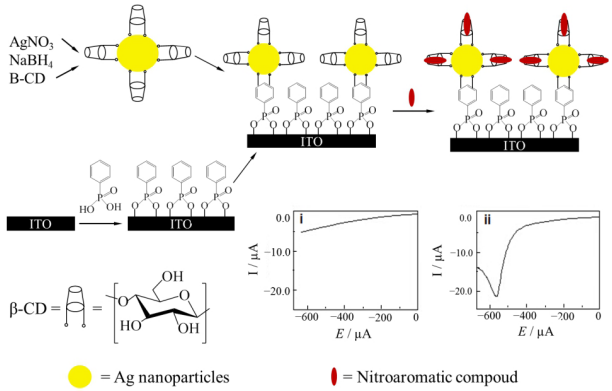


**Figure 5.** Schematic of the steps in the preparation of ITO/SAM/AgNPs/β-CD electrode for nitroaromatic compound isomers and the expected electrochemical responses (adapted from reference 10).

4-thiophenol modified electrode. The further attachment of biotin and anti-biotin IgG results in the increase in $R_{ct}$. The increase in $R_{ct}$ is linear to the concentration of anti-biotin IgG. The detection range for anti-biotin IgG was 5-500 ng mL$^{-1}$ with the detection limit as 5 ng mL$^{-1}$.[36] Later, the same group reported an increase in sophistication of the interface by adding an antifouling layer, oligo(ethylene glycol), to detect glycosylated hemoglobin HbA1c in human blood.[37] A competitive inhibition assay was employed where the surface bound glycosylated pentapeptide, an analogon to HbA1c, and HbA1c in solution compete for the anti-HbA1c IgG antibodies. The higher the concentration of HbA1c, the lesser antibody binds to the sensing interface and the lower the change of $R_{ct}$. The response of the immunosensor is linear with the HbA1c% of total haemoglobin in the range of 0-23.3%. The developed impedance-based immunosensor was used for the detection of HbA1c in human blood, and the result showed reasonably good agreement with that obtained from pathology. As progression of their work, Liu *el al.*[38] developed an amperometric HbA1c biosensor. Here the surface was passivated with oligo(ethylene glycol) to resist unwanted adsorption of protein in real sample (Figure 6). The main difference from the earlier work is that a surface bound ferrocene was used as a probe to read the concentration of HbA1c in the sample. Complexation of anti-HbA1c IgG with the surface bound epitope resulted in attenuation of the ferrocene electrochemistry and used to measure the concentration of HbA1c. This new amperometric immunosenosr was analogous to a previously prepared immunosensor by the same group where the surface was modified with an oligo(phenylethynylene) molecular wire and an oligo(ethylene glycol). The mixed layer is formed from *in situ*-generated aryl diazonium cations. To the distal end of the molecular wire, a redox probe [1,10-di(aminomethyl)ferrocene] was attached followed by the covalent attachment of *N*-glycosylated pentapeptide (epitope) to which an anti-HbA1c monoclonal antibody IgG binds selectively. We mention this study involving molecular wires as the electrode-organic layer-nanoparticle constructs shown in Figure 6 is a much simpler and robust way of making the same type of device as the molecular wires is demanding to synthesize and very unstable[39-41] while the nanoparticle interface is trivial to construct.

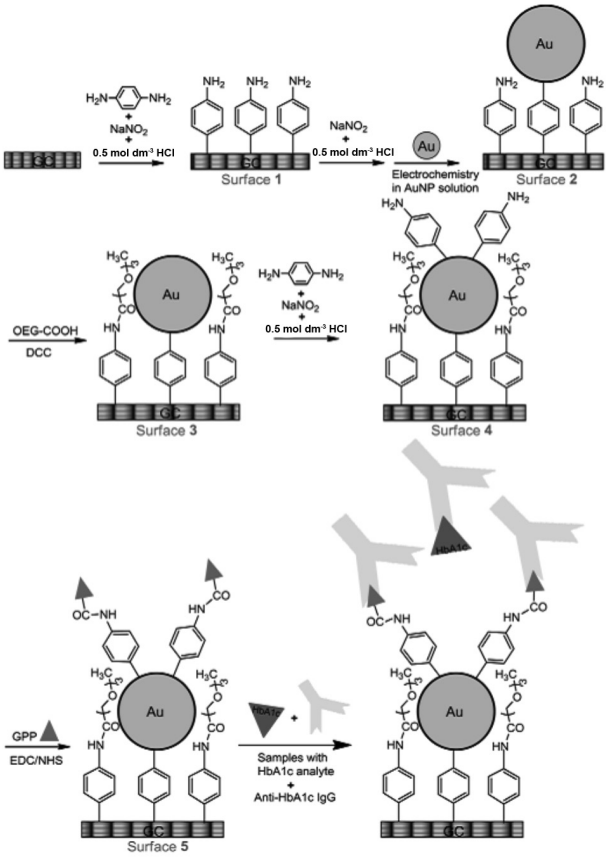


**Figure 6.** The schematic of fabrication of impedemetric immunosensor based on AuNP-diazonium salt modified sensing interface for the detection of HbA1c (Adapted from reference 33).

### 3.2 Photovoltaic cell

Quantum dot sensitized solar cells (QDSCs) or the so-called next generation solar cells have evolved in recent years due to the unique light harvesting properties of semiconductors. The ability to modulate the photoresponse by varying the size of quantum dot, simple synthetic procedure and sensitivity to diffused light have brought extra attention of the solar cell researchers to QDSCs. With the increased interest there arises a need to better understand how surface modification by quantum dots can affect the electron transfer across organic layers.

The extent of charge transfer mediation by nanoparticles in an insulating layer is determined by the overlap between

the density of states (DOS) of the nanostructures and the energy levels of a redox species in solution. The insulating layer behaves like a short circuit when the energy levels of the nanoparticles and redox species overlap efficiently. Kissling *et al.*[15,16] demonstrated this aspect by studying the effect of the progressive increment of the DOS of quantum dots towards the Fermi energy level of the redox species on the electron transfer kinetics. The DOS were varied by assembling quantum dots of different sizes and compositions. Quantum confinement effects as well as electron-hole coulombic interactions vary with particle size leading to a change in DOS of semiconducting particles.

A molecular layer of 11-mercaptoundecanoic acid (MUA) and poly(diallyldimethylammonium) (PDADMAC) was used as blocking layer by Kissling *et al.*[15] 3-mercaptopropionic acid stabilized quantum dots of different size were electrostatically attached on the blocking layer to study their effect on the electron transfer of the $[Fe(CN)_6]^{3-/4-}$ couple. Figure 7 illustrates the effect of adsorbed CdTe quantum dots on the redox behavior of $[Fe(CN)_6]^{3-/4-}$. The electrochemical response was substantially enhanced upon adsorption of the dots, particularly in the reduction reaction. Metal-like performance is observed with large quantum dot. Upon increasing the CdTe dot diameter from 2.1 to 3.6 nm,[16] the difference between the energy levels decreases from 340 to 6 meV. Similar outcome was obtained with CdSe quantum dot.[16] The key parameter determining the charge transfer mediation is the extent of overlap between the Fermi level of the redox species and the valence band of the nanostructures. With increasing size of CdTe, the valence band edge of quantum dot approaches the Fermi energy level of the $[Fe(CN)_6]^{3-/4-}$ hence, by regulating the radii of the quantum dot, the rate of electron transfer can be controlled. These observations are consistent with the dependence of the formal charge transfer resistance on the average dot size as probed by impedance spectroscopy.[15]

Electron transfer as a function of the distance between CdSe quantum dots and a gold electrode was studied by Kamat *et al.*.[42,43] To control this distance, they have used two classes of rigid and non-rigid molecular spacers. After absorption of a photon with energy larger than the band gap, a long-lived excited state can be formed if the hole from the highest occupied molecular orbital or the electron from the lowest occupied molecular orbital is trapped in a localized band-gap state. Electron transfer from the particle to the gold electrode can occur only when the gold Fermi level is below the electron level. The layer-by-layer assembled quantum dots multilayer sensitizer can offer unique opportunities in exploiting the size-dependent properties of quantum dots in light harvesting and in enhancing the charge collection efficiency.[44] The tandem-layered CdSeS (QDSSC) showed greater efficiencies than the values obtained from the corresponding devices of single quantum dot layered photoanodes. Multilayered QDSSCs can offer a unique opportunity to flexibly tune the light harvesting upon increasing the number of quantum dots layers and can also provide a controlled method of proximity between quantum dots, which is crucial for the sophisticated interactions between the adjacent quantum dot layers. Multilayered quantum dot sensitizers are expected to be suited well for the band-gap-controlled structure with facilitated electron and/or energy transfers.

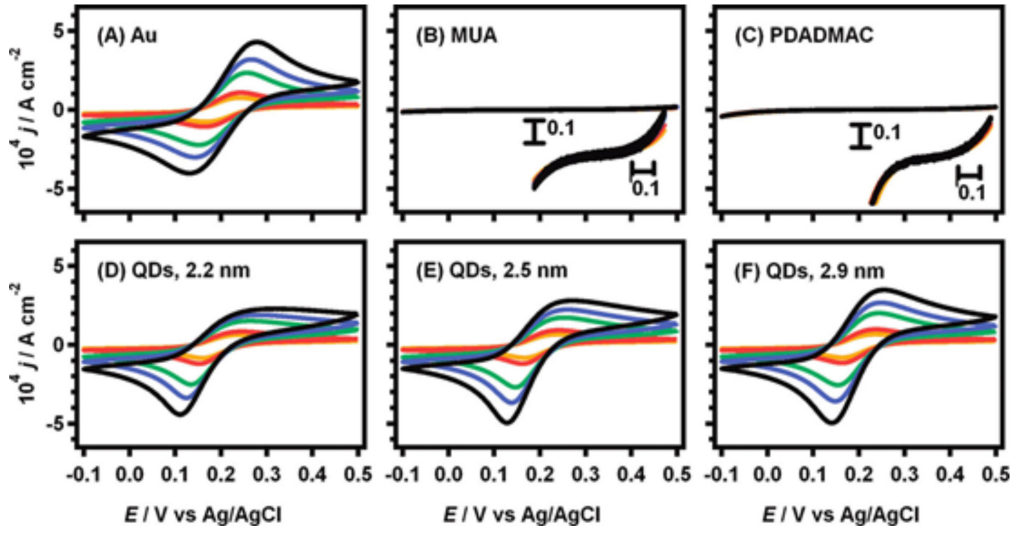


**Figure 7.** Cyclic voltammograms in the presence of $1.0 \times 10^{-3}$ mol dm$^{-3}$ $[K_4Fe(CN)_6]$ and $[K_3Fe(CN)_6]$ for a clean Au electrode (A) and after modification with MUA (B), MUA-PDADMAC (C) (insets representing 14× magnification), and MUA-PDADMAC quantum dots of 2.2 (D), 2.5 (E), and 2.9 nm (F) diameter. Voltammograms were measured at 5, 10, 50, 100, and 200 mV s$^{-1}$ (Adapted from reference 15).

## 4. Conclusions

The innovation of transforming passivated electrodes to desirable high efficient nanostructures by just decorating the modified surfaces with nanomaterials have attracted considerable research interest in the last few years. A thickness independent electron transfer that is observed for organic layers thinner than 20 Å makes these nanoparticle-constructs particularly attractive for a range of applications including electroanalysis, photovoltaics and electrocatalysis. The attractiveness is for several reasons. Firstly, the passivating organic layer means that the electrodes will have low background capacitance which facilitates low detection limits in electroanalysis. Secondly, as the density of the nanoparticles is easily controlled it is simply to fabricate nanoelectrode arrays where the electrochemistry approximates to a microelectrode with linear diffusion or can look more microelectrode like where radial diffusion dominates. Thirdly, the high density of states that can exist on the nanoparticles has an attractiveness for photovoltaics as does the fact that the energy levels of the nanoparticles are tuneable by altering the size of the nanoparticles. Finally, all the exquisite control we have over nanoparticle synthesis can now be translated to electrochemistry where the catalytic potential of specific nanoparticle crystal faces can be exploited for electrocatalysis in a very simple manner. In regards to electrocatalysis the first forays in this direction have recently been published[45] as has strategies to make very stable linkages between the nanoparticles and the organic layer.[8]

## Acknowledgements

Our research in this area was supported under Australian Research Council's Discovery Projects funding scheme (project number DP1094564) and the Linkage Projects funding scheme (project number LP100200593).

***Scientia Professor Justin Gooding*** *is the leader of the Biosensor and Biointerfaces Research Group at the University of New South Wales. He obtained a DPhil from Oxford University and post-doctoral training from the Institute of Biotechnology at Cambridge University. In 1997 he returned to his native Australia, joining the University of New South Wales. He was promoted to full Professor in 2005 and is currently an Australian Research Council Professorial Fellow. His research interests lie in biosensors, biointerfaces and surface chemistry.*

***Muhammad Tanzirul Alam*** *received his MSc from Shahjalal University of Science and Technology, Bangladesh in 2003 and DSc from Tokyo Institute of Technology, Japan in September 2008. He is currently working as post-doctoral fellow with Professor Justin Gooding at the University of New South Wales, Australia. His area of research interest includes modification of the electrode surface with different metal nanoparticles and biomolecules and their applications in oxygen reduction and biosensor. At present he is working on to develop an electrochemical sensor for the at-home monitoring of glycosylated haemoglobin (HbA1c) which is a biomarker to diagnose diabetes.*

***Abbas Barfidokht*** *is doing his PhD in the School of Chemistry at the University of New South Wales, Sydney, Australia since 2011. His current research is focused on fabricating an electrochemical biosensor for glycosylated hemoglobin (HbA1c) under the supervision of Professor Justin Gooding. Before that, he received his MSc degree from Institute for Advanced Studies in Basic Sciences (IASBS, Iran) in 2008.*

***Lachlan Carter*** *is a postgraduate student at the University of New South Wales. He completed his BSc (Chemistry) in 2011 at the University of New South Wales before working with BASF Construction Chemicals. He is currently undertaking a MPhil (Chemistry) with Professor Justin Gooding. His research aims to develop a new biosensor that combines the use of gold-coated magnetic nanoparticles and self-assembled monolayer modified electrodes.*

## References

1. Katz, E.; Willner, I.; Wang, J.; *Electroanalysis* **2004**, *16*, 19.
2. Freeman, R. G.; Grabar, K. C.; Allison, K. J.; Bright, R. M.; Davis, J. A.; Guthrie, A. P.; Hommer, M. B.; Jackson, M. A.; Smith, P. C.; Walter, D. G.; Natan, M. J.; *Science* **1995**, *267*, 1629.
3. Grabar, K. C.; Allison, K. J.; Baker, B. E.; Bright, R. M.; Brown, K. R.; Freeman, R. G.; Fox, A. P.; Keating, C. D.; Musick, M. D.; Natan, M. J.; *Langmuir* **1996**, *12*, 2353.

4. Bethell, D.; Brust, M.; Schiffrin, D. J.; Kiely, C.; *J. Electroanal. Chem.* **1996**, *409*, 137.
5. Brust, M.; Bethell, D.; Kiely, C. J.; Schiffrin, D. J.; *Langmuir* **1998**, *14*, 5425.
6. Horswell, S. L.; O'Neil, I. A.; Schiffrin, D. J.; *J. Phys. Chem. B* **2003**, *107*, 4844.
7. Le Saux, G.; Ciampi, S.; Gaus, K.; Gooding, J. J.; *ACS Appl. Mater. Interfaces* **2009**, *1*, 2477.
8. Liu, G.; Luais, E.; Gooding, J. J.; *Langmuir* **2011**, *27*, 4176.
9. Bradbury, C. R.; Kuster, L.; Fermin, D. J.; *J. Electroanal. Chem.* **2011**, *646*, 114.
10. Chen, X.; Cheng, X. Y.; Gooding, J. J.; *Anal. Chem.* **2012**, *84*, 8557.
11. Chen, X.; Chockalingam, M.; Liu, G.; Luais, E.; Gui, A. L.; Gooding, J. J.; *Electroanalysis* **2011**, *23*, 2633.
12. Diao, P.; Liu, Z. F.; *J. Phys. Chem. B* **2005**, *109*, 20906.
13. Su, L.; Gao, F.; Mao, L. Q.; *Anal. Chem.* **2006**, *78*, 2651.
14. Chou, A.; Eggers, P. K.; Paddon-Row, M. N.; Gooding, J. J.; *J. Phys. Chem. C* **2009**, *113*, 3203.
15. Kissling, G. P.; Bunzli, C.; Fermin, D. J.; *J. Am. Chem. Soc.* **2011**, *132*, 16855.
16. Kissling, G. P.; Miles, D. O.; Fermin, D. J.; *Phys. Chem. Chem. Phys.* **2011**, *13*, 21175.
17. Bradbury, C. R.; Zhao, J. J.; Fermin, D. J.; *J. Phys. Chem. C* **2008**, *112*, 10153.
18. Shein, J. B.; Lai, L. M. H.; Eggers, P. K.; Paddon-Row, M. N.; Gooding, J. J.; *Langmuir* **2009**, *25*, 11121.
19. Zhao, J.; Wasem, M.; Bradbury, C. R.; Fermin, D. J.; *J. Phys. Chem. C* **2008**, *112*, 7284.
20. Zhao, J. J.; Bradbury, C. R.; Fermin, D. J.; *J. Phys. Chem. C* **2008**, *112*, 6832.
21. Zhao, J.; Bradbury, C. R.; Huclova, S.; Potapova, I.; Carrara, M.; Fermin, D. J.; *J. Phys. Chem. B* **2005**, *109*, 22985.
22. Dyne, J.; Lin, Y. S.; Lai, L. M. H.; Ginges, J. Z.; Luais, E.; Peterson, J. R.; Goon, I. Y.; Amal, R.; Gooding, J. J.; *Chem. Phys. Chem.* **2010**, *11*, 2807.
23. Bharathi, S.; Nogami, M.; Ikeda, S.; *Langmuir* **2001**, *17*, 7468.
24. Chazalviel, J. N.; Allongue, P.; *J. Am. Chem. Soc.* **2011**, *133*, 762.
25. Ikeda, K.; Fujimoto, N.; Uehara, H.; Uosaki, K.; *Chem. Phys. Lett.* **2008**, *460*, 205.
26. Barfidokht, A.; Ciampi, S.; Luais, E.; Darwish, N.; Gooding, J. J.; *Anal. Chem.* **2013**, *85*, 1073.
27. Barfidokht, A.; Ciampi, S.; Luais, E.; Darwish, N.; Gooding, J. J.; *Chem. Phys. Chem.* **2013**, *14*, 2190.
28. Liu, F.; Khan, K.; Liang, J. H.; Yan, J. W.; Wu, D. Y.; Mao, B. W.; Jensen, P. S.; Zhang, J.; Ulstrup, J.; *Chem. Phys. Chem.* **2013**, *14*, 952.
29. Smalley, J. F.; Feldberg, S. W.; Chidsey, C. E. D.; Linford, M. R.; Newton, M. D.; Liu, Y. P.; *J. Phys. Chem.* **1995**, *99*, 13141.
30. Jensen, P. S.; Chi, Q.; Grumsen, F. B.; Abad, J. M.; Horsewell, A.; Schiffrin, D. J.; Ulstrup, J. *J. Phys. Chem. C* **2007**, *111*, 6124.
31. Jensen, P. S.; Chi, Q.; Zhang, J.; Ulstrup, J. *J. Phys. Chem. C* **2009**, *113*, 13993.
32. Cheng, W. L.; Dong, S. J.; Wang, E. K.; *Langmuir* **2002**, *18*, 9947.
33. Cheng, W. L.; Dong, S. J.; Wang, E. K.; *Anal. Chem.* **2002**, *74*, 3599.
34. Gooding, J. J.; Shein, J.; Lai, L. M. H.; *Electrochem. Commun.* **2009**, *11*, 2015.
35. Raj, M. A.; Revin, S. B.; John, S. A.; *Colloids Surf. B* **2011**, *87*, 353.
36. Liu, G.; Liu, J.; Davis, T. P.; Gooding, J. J.; *Biosens. Bioelectron.* **2011**, *26*, 3660.
37. Liu, G. Z.; Iyengar, S. G.; Gooding, J. J.; *Electroanalysis* **2012**, *24*, 1509.
38. Liu, G. Z.; Iyengar, S. G.; Gooding, J. J.; *Electroanalysis* **2013**, *25*, 881.
39. Liu, G. Z.; Gooding, J. J.; *Langmuir* **2006**, *22*, 7421.
40. Liu, G. Z.; Paddon-Row, M. N.; Gooding, J. J.; *Chem. Commun.* **2008**, *33*, 3870.
41. Liu, G. Z.; Khor, S. M.; Iyengar, S. G.; Gooding, J. J.; *Analyst* **2012**, *137*, 829.
42. Douglas, A. H.; Kamat, P. V.; *J. Phys. Chem. C* **2013**, *117*, 14418.
43. Kamat, P. V.; *J. Phys. Chem. C* **2008**, *112*, 18737.
44. Jin, H.; Choi, S.; Lee, H. J.; Kim, S.; *J. Phys. Chem. Lett.* **2013**, *4*, 2461.
45. Mertens, S. F. L.; Bütikofer, A.; Siffert, L.; Wandlowski, T.; *Electroanalysis* **2010**, *22*, 2940.

*Submitted: August 21, 2013*
*Published online: December 19, 2013*